European Journal of Medicinal Chemistry 64 (2013) 260–272

Contents lists available at SciVerse ScienceDirect

European Journal of Medicinal Chemistry

journal homepage: http://www.elsevier.com/locate/ejmech

Original article

A potential antitumor agent, (6-amino-1-methyl-5-nitrosouracilato-N3)-triphenylphosphine-gold(I): Structural studies and *in vivo* biological effects against experimental glioma

Nuria A. Illán-Cabeza [a], Antonio R. García-García [a], José M. Martínez-Martos [b], María J. Ramírez-Expósito [b], Tomás Peña-Ruiz [c], Miguel N. Moreno-Carretero [a,*]

[a] Department of Inorganic and Organic Chemistry, University of Jaén, Spain
[b] Department of Health Sciences, University of Jaén, Spain
[c] Department of Physical and Analytical Chemistry, University of Jaén, Spain

ARTICLE INFO

Article history:
Received 14 November 2012
Received in revised form
29 March 2013
Accepted 30 March 2013
Available online 10 April 2013

Keywords:
Gold
Uracil
Pyrimidine
Antioxidant
Antitumor activity

ABSTRACT

The synthesis and molecular and supramolecular structures of the compound (6-amino-1-methyl-5-nitrosouracilato-N3)-triphenylphosphine-gold(I) with interesting abilities to inhibit tumor growth in an animal model of experimental glioma are reported. Thus, its antitumor properties, effects on both enzyme and non-enzyme antioxidant defense systems and the response of several biochemical biomarkers have been analyzed. After seven days of treatment, the gold compound decreased the tumor growth to *ca.* one-tenth and reduced oxidative stress biomarkers (thiobarbituric acid-reactive substances (TBARS) and protein oxidation levels) compared to animals treated with the vehicle. Also, gold compound maintained non-enzyme antioxidant defense systems as in non-tumor animals and increased enzyme antioxidant defenses, such as superoxide dismutase and glutathione peroxidase activities, and decreased catalase activity. Analysis of serum levels of electrolytes, nitrogenous compounds, glucose, lipids, total protein, albumin, transaminases and alkaline phosphatase indicated that gold compound treatment showed few adverse effects, while effectively inhibiting tumor growth through mechanisms that involved endogenous antioxidant defenses.

© 2013 Elsevier Masson SAS. All rights reserved.

1. Introduction

Malignant gliomas, the most frequent brain tumors, are currently non-curable central nervous system neoplasias and unfortunately there has been little improvement in the efficacy of adjuvant therapies [1,2]. Brain tumorigenesis is associated with oxidative stress. This is reflected by an imbalance between free radicals production and antioxidant mechanism. In pathological conditions, free radicals are generated in excess from endogenous sources such as mitochondria, peroxisomes, inflammatory cell activation or neurotransmitters oxidation, and exogenous sources, including environmental agents, drugs, irradiation or chemicals. The resulting oxidative stress promotes various pathologic reactions which contribute to illness. In response to various inducers, large amounts of free radicals (superoxide anion, hydrogen peroxide and hydroxyl groups) trigger lipid peroxidation of the cellular membranes, oxidation of proteins and DNA and lead to changes in chromosome structure, genetic mutations and/or modulation of cell growth. In fact, it was shown that oxygen-derived free radicals play an important role in tumor development. Although the induction of cancer represents a multistage, multistep process, involving multiple molecular and cellular events, the transformation of a normal cell into a malignant one, initiation, promotion and progression stages have been described [3,4]. But brain tumor development involves not only oxidative aggression but also a reduced response of antioxidant defense. During prolonged oxidative stress, changes in brain non-enzyme (reduced glutathione, GSHr) and enzyme antioxidant activities

Abbreviations: GSHr, glutathione reduced; GSSG, glutathione disulfide; SOD, superoxide dismutase; GPx activity, glutathione peroxidase activity; TBARS, thiobarbituric acid reactive substances; MDA, malondialdehyde; CAT, catalase; ASP, aspartate aminotransferase; ALT, alanine aminotransferase; ALP, alkaline phosphatase.

* Corresponding author. Dpto. Química Inorgánica y Orgánica, Universidad de Jaén, Campus Las Lagunillas B3, 23071 Jaén, Spain. Tel.: +34 953212738; fax: +34 953211876.
E-mail addresses: mmoreno@ujaen.es, m.moreno.carretero@gmail.com (M.N. Moreno-Carretero).

0223-5234/$ – see front matter © 2013 Elsevier Masson SAS. All rights reserved.
http://dx.doi.org/10.1016/j.ejmech.2013.03.067

(superoxide dismutase, SOD, catalase and glutathione peroxidase, GPx), appear. These enzyme and non-enzyme systems act to prevent or decrease brain damages caused by free radicals in excess. However, they are controlled by polymorphic genes which can be altered by free radicals, leading to dysfunctions.

A critical step in introducing clinical trials of treatments for gliomas after in vitro studies is to examine the efficacy and toxicity *in vivo* animal models. In studying malignant gliomas, rat C6 glioma models are widely used to evaluate the effects of novel therapies [5–8].

Gold and its complexes have been known to display unique biological and medicinal properties [9]. Specifically, gold(I) complexes exhibit significant biological properties that can be used for the development of novel therapeutic agents. Particularly important are the studies on gold(I)–phosphine complexes since the discovery of auranofin, because of their anticancer activity, especially in some cisplatin-resistant cell lines. The mechanisms of action of anticancer gold(I) and gold(III) complexes appear in general to be DNA independent and essentially cisplatin unrelated. Several proteins with important functional roles in cells are effective targets for cytotoxic gold compounds, such as thioredoxin reductase [10], cathepsins [11], tyrosine phosphatase [12], proteasomes [13], iodothyronine deiodinase [14] and, recently, zinc finger proteins such as PARP-1 [15]. The different mechanisms which contribute to the pharmacological profile of gold complexes are based on their different ligands, different kinetic properties, geometries and other features [9,16–18]. A possible therapy in the treatment of cancer could be through the potentiation of antioxidant defenses.

In previous reports the evaluation of the biological properties against different tumoral cell lines in metalated uracils have been carried out with interesting results [19–21]. Thus, in the present work, we report the structure of a new gold(I) compound, [Au(MANUH$_{-1}$)(PPh$_3$)], containing 6-amino-1-methyl-5-nitrosouracilato ligand (MANUH$_{-1}$) binding the metal in a quite unusual monodentate N3 mode, and its antitumor properties in an animal model glioma. Also, we describe its effects on both non-enzyme and enzyme antioxidant defense systems and on several biochemical serum biomarkers, to analyze putative adverse effects of the treatment in several physiological functions.

2. Chemistry of [Au(MANUH$_{-1}$)PPh$_3$]

2.1. Synthesis and spectral characterization

The synthesis of the precursor organic ligand 6-amino-1-methyl-5-nitrosouracil (MANU) was already described (Scheme 1) [21]. The complex [Au(MANUH$_{-1}$)PPh$_3$] was obtained by mixing [AuCl(PPh$_3$)] and MANU (1:4) in a methanolic alkaline medium. Precursor and gold complex were characterized by IR, MS and NMR spectra. The IR spectra display the bands due to the endocyclic carbonyl groups which appear at around 1729 and 1705 cm^{-1} in the free ligand, whereas in the complex they are shifted to lower wavenumber (about 50–90 cm^{-1}); these bands are primarily sensitive to the loss of the pyrimidine proton H3. In the 600–200 cm^{-1} range, the stretching vibration associated to M–P has been assigned in accordance with data found in literature [22]. EI-MS shows the peak of the monoprotonated specie [M$^+$] at *m*/*z* 629 and those of the corresponding loss of MANU and Au–MANU fragments.

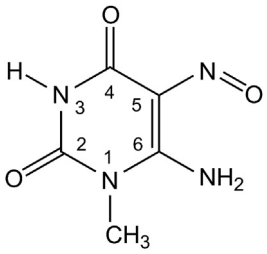

Scheme 1. Structure of the 6-amino-1-methyl-5-nitrosouracil (MANU) showing the IUPAC's numbering system.

On comparing the ^{1}H NMR spectra of both metalated and free-metal ligand, the most remarkable feature is the disappearance of the signal corresponding to the H3 proton. ^{13}C NMR data show a general deshielding as consequence of the nitrogen N3 coordination, with important downfield shifts for the signals assignable to C2 and C4 carbon atoms due to their proximity to N3 atom (5–7.5 ppm). Double signals in CP–TOSS spectra are observed for C1 and C2 atoms due to an insufficient rotation which induces the splitting of the signals [23]. The ^{31}P{^{1}H} NMR spectrum of the complex displays a singlet at 31.38 ppm, which is downfield shifted *ca.* 1 ppm with respect to its position in the [AuCl(PPh$_3$)] spectrum; this signal is very close to those found for other triphenylphosphine complexes containing the N–Au–P fragment [24,25]. In order to check the stability of the title compound in DMSO solution and bearing in mind that the treatments of animals were performed along one week, the ^{1}H NMR spectrum (DMSO) was recorded at intervals of two days during ten days; the spectra indicate no significant decomposition.

2.2. XRD single-crystal study

The crystal structure of [Au(MANUH$_{-1}$)PPh$_3$]·¼H$_2$O obtained by X-ray diffraction analysis consists in asymmetric units containing two independent and virtually identical molecules; one of them is shown in Fig. 1. The Au(I) center is coordinated by a deprotonated endocyclic N3 atom of the MANU ligand and the phosphorus of a triphenylphosphine, displaying a typical quasi-linear geometry with P–Au–N angles of 169.3(2) and 173.2(2)°. The distances Au–P (2.215(2) and 2.218(2) Å) and Au–N (2.058(5) and 2.057(5) Å) are similar to those found in other P–Au–N compounds [26–28].

The uracil ligand is roughly planar and coordinates to the metal in a quite unusual monodentate N3 binding mode, this behavior is also observed in complexes with 1-methylthymine or 1-methylcytosine which often act as bidentate ligands through the deprotonated N3 atom but also the partially enolyzed O4 atom [29–31]. Despite an extensive electronic delocalization existing, the MANUH$_{-1}$ anion can be best described as a 6-amino-5-nitroso-2,4-dioxo

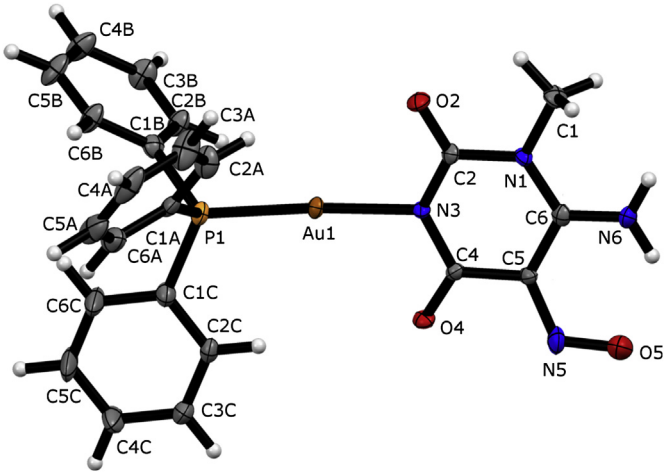

Fig. 1. ORTEP plot of one [Au(MANUH$_{-1}$)PPh$_3$] molecule (ellipsoids at 30% probability).

tautomeric form in which the negative charge mainly lies in the N3 atom [32].

Both [Au(MANUH$_{-1}$)PPh$_3$] molecules from the asymmetric residual unit are dimerized through three different interactions (see Fig. 2), being mutually assembled by N3–Au1–Au2–N3′ and P1–Au1–Au2–P2 dihedral angles of 75.1(5) and 72.2(5)°, respectively. First of all, there are weak aurophilic Au···Au interactions (3.255(1) Å). In addition to this, π–π stacking contacts between phenyl rings from the PPh$_3$ ligands (*d*(Cg–Cg), 3.562(2) Å; *α*, 4.1(5)°; *β* and *γ*, 9.1(5)°; slippage *ca.* 0.56 Å) and σ–π interactions involving the C4–O4 carbonyl oxygen and the uracil ring of the other crystallographically independent molecule (*d*(O4–Cg), 2.896(5) and 3.202(5) Å; *α*(C4–O4–Cg), 104.8(4) and 97.3(4)°) contribute to the stabilization of the cluster [33]. The crystal structure grows forming chains parallel to the *b* axis. Inside them, the Au–uracil polar residues are H-bonded involving the 5-nitroso and 6-amino groups and the disordered crystallization water molecule, whereas the lipophilic phenyl groups are oriented outward.

2.3. Computational chemistry

An objective of the present work is the qualitative characterization of the link among the ligands MANU and PPh$_3$ with the gold atoms as well as the interactions (Au···Au and others) in the binuclear cluster [Au(MANUH$_{-1}$)PPh$_3$]$_2$. This task is accomplished by the topological analysis of the electronic density within the frame of Bader's Atoms in Molecules theory [34].

The data to characterize the main stabilizing interactions appearing in the binuclear [Au(MANUH$_{-1}$)PPh$_3$]$_2$ complex are shown in Table 1. As it is observed, the BCPs among the ligands and the gold atoms as well as between the gold atoms themselves exhibit a positive value of the Laplacian, i.e., the electronic charge is shifted toward the maxima centered at the atoms, demonstrating that these interactions are closed shell (non-covalent) in nature. Also, it is observed the electronic density for the BCP of the interaction Au···Au is one order of magnitude lower than that one for Au···N and Au···P leading to the conclusion that the former link is weaker than the latter, which is consistent with the length of distance between both gold atoms since it is close to the sum of the Van der Waals radii (3.32 Å).

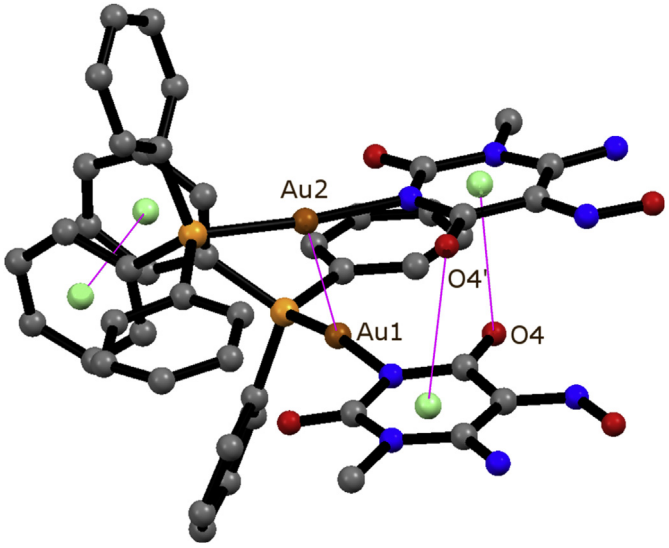

Fig. 2. A view of the asymmetric residual unit showing, left to right, the dimerization by π–π (3.562(2) Å), Au–Au (3.255(1) Å) and σ–π C4–O4···Cg (3.202(5) and 2.896(5) Å) intermolecular interactions (centroids are drawn as green balls). Hydrogen atoms are omitted for clarity. (For interpretation of the references to color in this figure legend, the reader is referred to the web version of this article.)

Table 1
Topological parameters for the bond critical points (BCP) appearing in the [Au(MANUH$_{-1}$)PPh$_3$]$_2$ dimer.

Interaction (BCP)	TPSS			LC–TPSS		
	ρ	ε	$\nabla\rho$	ρ	ε	$\nabla\rho$
Major						
Au···N	0.119	0.059	0.393	0.120	0.050	0.400
Au···P	0.131	0.013	0.061	0.132	0.013	0.072
Au···Au[a]	0.020	0.034	0.049	0.018	0.047	0.051
Minor						
Au···(O2=C2)[a]	0.008	0.216	0.025	0.008	0.176	0.025
Au···(H–C$_{ph}$)[a]	0.006	0.269	0.017	0.005	0.275	0.017
C2=O2···(H–C$_{ph}$)[a]	0.011	0.044	0.037	0.009	0.030	0.032
C$_{ph}$···C$^a_{ph}$	0.005	2.724	0.014	0.005	3.056	0.014
C4=O4···C4[a]	0.009	0.719	0.033	0.009	2.648	0.030
N5···N5[a]	0.003	0.111	0.011	0.003	0.269	0.011
C2=O2···C$^a_{ph}$	0.003	0.454	0.012	0.004	0.525	0.012
C$_{ph}$–H···C$_{ph}$	0.009	0.735	0.032	0.009	0.892	0.032

[a] Starred atoms or groups belong to the neighbor mononuclear complex. Otherwise, the interaction is intra-mononuclear complex.

Other BCPs characterizing weaker interactions which contribute to stabilize the structure of the binuclear complex are found in the topological analysis. Accordingly, they show lower values of the electronic density. Also, those of π–π nature exhibit high ellipticity what it is in agreement with the delocalization of the electrons. Finally, some weak Au···H interactions have been detected for both density functionals.

3. Biological studies

3.1. Antiproliferative effects of [Au(MANUH$_{-1}$)PPh$_3$] in vitro

There is growing evidence suggesting that antioxidants may be useful in treating primary brain tumors. A dynamic relationship exists between oxidative stress and brain tumor appearance, with tumor microenvironment being a key player in the neoplastic process. In the present report we describe for the first time the effects of the treatment with a new compound against glioma, both in vitro and *in vivo*. In vitro, we show the dose–effect relationship of [Au(MANUH$_{-1}$)PPh$_3$] on the growth of C6 glioma cells and determine its potency (Dm), through the median–effect analysis, shape (*m*), and conformity (*r*) (Table 2). It is clear that the tested compound is a potent cytotoxic agent on C6 glioma cells, showing a Dm (IC50) value *ca.* 3 μM.

3.2. Antitumor effects of [Au(MANUH$_{-1}$)PPh$_3$] in vivo

The effects *in vivo* of seven days of administration of [Au(MANUH$_{-1}$)PPh$_3$] on tumor growth in our experimental glioma

Table 2
Dose–effect relationship parameters of [Au(MANUH$_{-1}$)PPh$_3$] on growth of C6 glioma cells.[a]

Drug dosage (μM)	Fa[b]	*m*[b]	Dm (μM)[b]	*r*[b]
2	0.209			
4	0.818			
6	0.839			
8	0.869			
10	0.868	1.949	2.93	0.897

[a] Method of cytotoxicity assay is described in Experimental section.
[b] The parameters Fa, *m*, Dm and *r* are the fractional inhibition, slope coefficient of the curve, dose at 50% inhibition (equivalent to IC50 value), and the linear correlation coefficient of the median–effect plot.

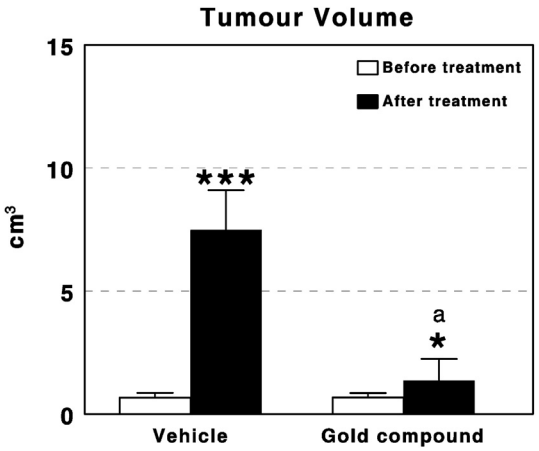

Fig. 3. Growth curve of implanted C6 glioma tumor volumes implanted at the subcutaneous region treated with vehicle or with 20 μL of [Au(MANUH$_{-1}$)PPh$_3$] 6.5 mM during seven days. Results are expressed in cm^3 (Mean ± SEM; $n = 8$ animals per group; $^{***}P < 0.001$).

model compared with the vehicle-treated only are presented in Fig. 3. The tumor volume on non-treated animals increased significantly ($P < 0.001$) by 1030%, from 0.66 ± 0.20 cm^3 to 7.47 ± 1.62 cm^3. On the contrary, animals treated with gold(I) complex showed a significant tumor volume increase ($P < 0.05$) by only 103%, from 0.67 ± 0.18 to 1.36 ± 0.88 cm^3. Therefore, the treatment during a week with [Au(MANUH$_{-1}$)PPh$_3$] significantly decreased the tumor growth ($P < 0.001$) to *ca.* one-tenth.

About their histopathological characteristics (Fig. 4), non-treated animals show central necrosis in the tumor tissue in some areas, revealing the presence of tumor cells invading the subcutaneous tissue as well as infiltration of the skin cells in the tumor. In the image, atypical cells in loosely cohesive clusters with nuclear pleomorphisms and intranuclear inclusion are found in large areas. Polygonal to spindle-shaped cells also appear and fibrillary processes extending from the atypical cells were apparent. Also, it can be observed the tumor area infiltration with cellular atypia showing abundant cellularity and necrosis. On the contrary, in treated animals, these effects are clearly diminished, also supporting the antitumor effect of the treatment with [Au(MANUH$_{-1}$)PPh$_3$].

3.3. *Effects of [Au(MANUH$_{-1}$)PPh$_3$] administration on oxidative stress parameters lipid peroxidation and protein oxidation*

We have found increased levels of the oxidative stress parameters lipid peroxidation (through the analysis of TBARS content, $P < 0.001$, Fig. 5) and protein oxidation (through the analysis of carbonyl and diene-conjugate groups content, $P < 0.001$, Fig. 6) in animals with glioma tumors treated with vehicle only, when compared with non-tumor healthy control animals. Otherwise, animals treated with [Au(MANUH$_{-1}$)PPh$_3$] also showed increased levels of TBARS (when compared with non-tumor control group), although significantly ($P < 0.05$) lower levels when compared with animals with glioma tumors. Regarding to protein oxidation, animals treated with the gold(I) compound showed similar values than non-tumor healthy control animals.

It is well known that lipid peroxidation is an early biomarker of oxidative damage, and is particularly damaging because of the wider propagation of free radicals associated with it. The elevated oxidative stress in cells can lead to modification of a number of cellular targets and cause cell damage and death; the subsequent lack of cellular repair processes has been associated with carcinogenesis [35,36]. It has long been documented that cancer cells are under increased and persistent oxidative stress due to elevated generation of intracellular free radicals. Increased oxidative stress and lipid peroxidation are implicated in carcinogenic processes [37–39]. The magnitude of this damage (called oxidative stress or oxidative damage) depends not only on free radical levels but also on the body's defense mechanisms against them mediated by various cellular antioxidants. High levels of oxidative stress result in peroxidation of membrane lipids with the generation of peroxides that can decompose to multiple mutagenic aldehyde products as malondialdehyde (MDA) which is used as a marker of oxidative stress in recent years studying the role played by lipid peroxidation in cancer progression. MDA is low-molecular weight aldehyde that can be produced from free radical attack on polyunsaturated fatty acids and in practice, TBARS are expressed in terms of malondialdehyde (MDA) equivalents [40]. The levels of TBARS reflect the extent of lipid peroxidation. An enhanced lipid peroxidation is considered to be mutagenic and carcinogenic [41]. Enhanced lipid peroxidation has been reported in benign brain disease compared with brain tumor [42,43]. Observations similar to our findings have been reported in studies on various human cancers [44–46] and TBARS has been used as a common oxidative stress biomarker. The results of our study are consistent with the findings of previous studies. Zengin et al. [47] observed increased levels of TBARS in tumor tissue samples when compared with peritumoral areas, which could be attributed to increased formation or inadequate clearance of free radicals by the cellular antioxidants. In astrocytoma, meningioma, metastatic and other type of tumors, TBARS levels were significantly higher when compared with their corresponding peritumoral adjacent tissue. In addition, important differences were observed when astrocytoma tumor group was compared with other tumor groups. When TBARS levels of low-grade and high-grade tumors were compared, it was clearly seen that lipid peroxidation was significantly higher in high-grade tumors. Elevated levels of lipid peroxidation products support the hypothesis that the tumoral cells produce large amounts of free radicals demonstrating a relationship between free radical activity and carcinogenesis. Also, it was shown in some studies that lipid peroxidation state depends on the tumoral area studied; when lipid peroxidation was estimated in low-grade and high-grade astrocytomas [48], TBARS values for low-grade astrocytomas were significantly elevated compared to those for malignant lesions, especially on the tumor surface and when energetic and oxidant metabolisms were explored in low-grade gliomas obtained from the center and the periphery of tumors [49] and it was seen lipid peroxidation was increased in the periphery compared to the center of tumors. Cirak studied lipid peroxidation levels in the serum as well as in the tissue samples of patients with high and low-grade glial tumors, showing that patients with high-grade tumors had higher MDA levels both in sera and tissue samples compared to low grades and controls [50]. This result implies the possibility that measurement of TBARS/MDA may be used as a marker of high lipid peroxidation associated with the metabolism of brain tumors [50], which support our findings. Although the results of this study in non-treated animals show higher lipid peroxidation levels in high-grade tumors contrary to the study of Louw et al. [48], it is in agreement with other studies performed, so a direct metabolic relationship can be hardly argued among brain tissues. However, in animals treated with the new compound [Au(MANUH$_{-1}$)PPh$_3$] we found decreased levels of TBARS when compared with non-treated animals, although certain levels of lipid peroxidation remained when compared with healthy animals. Also, they showed similar levels of carbonyl groups content than control animals. Taking into account that several products of lipid peroxidation are responsible of protein oxidation [51], the treatment with [Au(MANUH$_{-1}$)PPh$_3$]

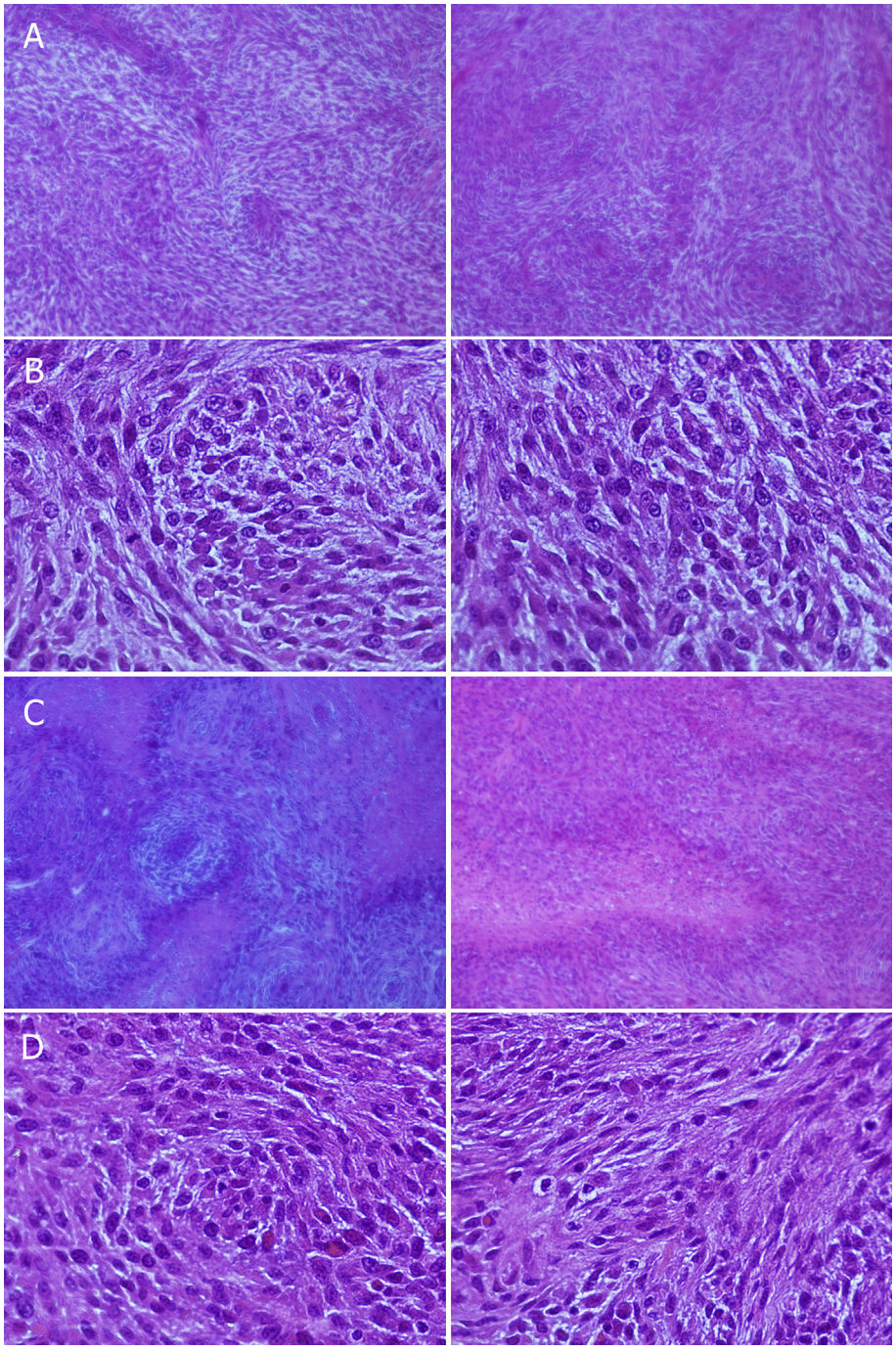

Fig. 4. Image showing histopathological characterization of two samples (right and left) of C6 glioma tumors implanted at the subcutaneous region treated with vehicle (A – 10× magnification; B – 40× magnification) or with 20 μL of [Au(MANUH$_{-1}$)PPh$_3$] 6.5 mM (C – 10× magnification; D – 40× magnification) during seven days.

reduced lipid peroxidation sufficiently to completely avoid protein oxidation.

3.4. Effects of [Au(MANUH$_{-1}$)PPh$_3$] administration on non-enzyme antioxidant defense systems

Despite Au itself not showing any antioxidant effect, we have found that [Au(MANUH$_{-1}$)PPh$_3$] acts by potentiating the endogenous antioxidant defense systems in our animal model of experimental glioma [52]. Thus, Fig. 7 shows the levels of reduced GSH (GSHr), GSSG, total GSH and the GSSG/GSHr ratio in serum of healthy animals (control group) treated with the vehicle, and animals with glioma treated with [Au(MANUH$_{-1}$)PPh$_3$] or with vehicle only. As it can be observed in the figure, there was a decrease of non-enzyme defense systems in animals with glioma when compared with non-tumor control group. Cellular antioxidants and free radical scavengers protect the cell against toxic levels of oxygen radicals. One of them is GSH, an important non-protein thiol. A significant depletion of GSH levels in astrocytoma, meningioma, metastatic and other types of brain tumors was found when compared with their peritumoral tissues. This depletion was probably related to the enhanced pro-oxidant milieu and correlated with increased lipid peroxides in the cranial neoplasms. Our results also agreed with Navarro et al. in that changes in glutathione status

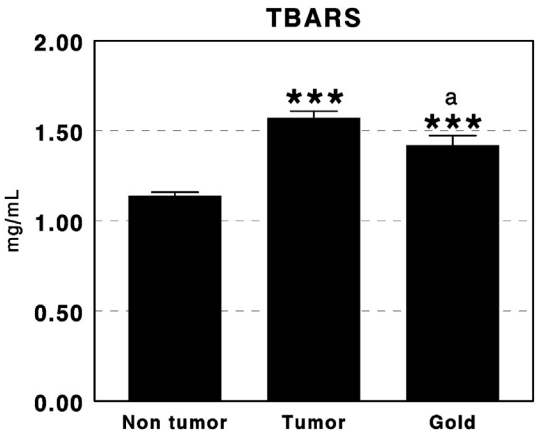

Fig. 5. Thiobarbituric acid reactive substances (TBARS) content in serum of non-tumor healthy control animals treated with vehicle, and animals with C6 glioma implanted at the subcutaneous region treated with vehicle or with 20 μL of [Au(MANUH$_{-1}$)PPh$_3$] 6.5 mM during seven days. Results are expressed in mg/mL (Mean ± SEM; $n = 8$ animals per group; $^{***}P < 0.001$).

and the antioxidant system in blood and in cancer cells were associated with tumor growth *in vivo* [53] and the GSH/GSSG ratio was reduced. This can be explained as the higher GSSG levels were due to the increase in the H_2O_2 production by the tumor, as well as to the changes in the activity of the glutathione-related antioxidant enzymes. Regarding our results, we have found that the treatment of animals with glioma tumors with the new Au(I) compound has important effects on non-enzyme antioxidant defense system. Thus, treated animals showed similar levels of GSHr, total GSH and GSSG/GSHr index compared to non-tumor healthy control animals, although the levels of GSSG remained high, also as a consequence of the pro-oxidant milieu. Therefore, [Au(MANUH$_{-1}$)PPh$_3$] treatment induced adequate levels of GSH despite the increase in oxidative processes and GSSG formation occurred as a consequence of glioma tumors.

3.5. Effects of [Au(MANUH$_{-1}$)PPh$_3$] administration on enzyme antioxidant defense systems

During prolonged oxidative stress, changes in antioxidant enzyme activities SOD, CAT and GPx appear. These enzymes

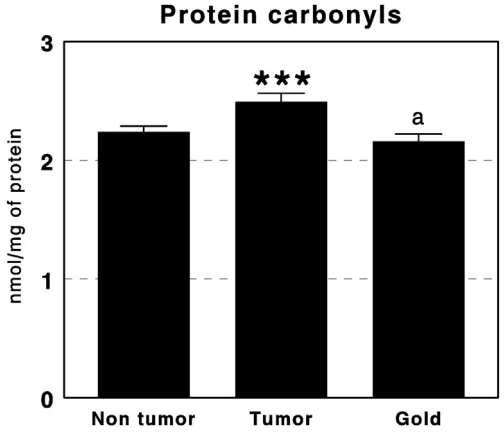

Fig. 6. Carbonyl groups content in serum of non-tumor healthy control animals treated with vehicle, and animals with C6 glioma implanted at the subcutaneous region treated with vehicle or with 20 μL of [Au(MANUH$_{-1}$)PPh$_3$] 6.5 mM during seven days. Results are expressed in nmol/mg of protein (Mean ± SEM; $n = 8$ animals per group; $^{***}P < 0.001$).

normally act to prevent or decrease tissue damages caused by free radicals. Animals with glioma tumors showed significant increased levels of SOD ($P < 0.001$) compared with the healthy control group (Fig. 8). However, data obtained for the animals treated with the gold(I) complex indicated even more increased levels of SOD activity ($P < 0.001$) than animals with tumors. Our results do not agree with the results of other authors [54,55] that showed that levels of SOD were significantly less in brain tumor cases than in controls. Another study also showed a proportionate decrease of SOD activity with increasing grades of malignancy in brain tumors [39]. Finally, SOD activity was also found to be lower in astrocytomas, meningiomas, metastatic tumors and other types of tumors when compared with their peritumoral tissues [47]. However, Del Maestro et al. reported that human glioma cells generally have relatively higher SOD activity compared with other tumor types, which seems to violate the general observation of low SOD activity in tumor cells [56]. This exception can probably be explained by the fact that the brain is well known as an organ with high levels of oxygen consumption. There is high production of superoxides during normal aerobic metabolism in the brain cells. Thus, relatively high levels of SOD and other antioxidant enzymes are required to remove high levels of free radicals in order to protect against damage to brain tissues. Although the levels of SOD are important to protect against oxidative damage, a balance of antioxidant enzymes is probably more important, as well as their levels, which may influence intracellular oxidative states. In any case, most of the studies present a significant reduction in SOD activity in several brain tumor types such as glioma, meningioma and metastatic tumors.

We did not find differences in the levels of catalase activity between non-tumor healthy control animals and animals with glioma tumors treated with the vehicle only (Fig. 9). Several authors have described changes in catalase activity with brain tumors. Thus, Yilmaz has described that catalase activity was significantly higher for both glial and meningiomal tumor cases when compared to controls [57]. In the same way, Popov has described that catalase activity in brain tumor tissue was 106.3% higher than that obtained in controls [54]. However, animals treated with [Au(MANUH$_{-1}$)PPh$_3$] showed significantly decreased levels of catalase activity ($P < 0.001$) when compared with control animals or animals with tumors, suggesting that the treatment blocks the role of catalase in converting H_2O_2 to H_2O.

Taking into account that conversion from H_2O_2 to H_2O could be also performed by GPx, we have analyzed this enzyme activity. Fig. 10 shows higher levels of GPx activity ($P < 0.001$) in animals treated with the title compound whereas it decreased in animals with glioma tumors ($P < 0.001$) compared to the control group. These data also explain the lower antioxidant capacity of the antioxidant system against free radicals, as well as the lower levels of GSHr and the higher values of GSSG/GSHr index. Other authors have found diminished levels of GPx in brain tumors [42,55,58]. Furthermore, when the authors separated the cases on the basis of histopathological kind of tumor, GPx showed a significant decrease as the tumor became more malignant [55]. The low levels of antioxidants in brain tumors could be a result of increased oxidative damage or it could be that low values aggravated the free radical damage and increased the chance of developing cancer, indicating antioxidants' role in prevention and the role of oxidative injury in the causation of cancer. The increase in GPx in the animals treated with the Au(I) complex explained the increased levels of GSHr obtained with the treatment, and also implicate that an increase in the enzyme antioxidant defense system mediated by this enzyme activity occurred with SOD. Therefore, it seems that the ability of scavenging oxygen free radicals was impaired in animals with glioma tumors because of the lowered levels of antioxidants, which

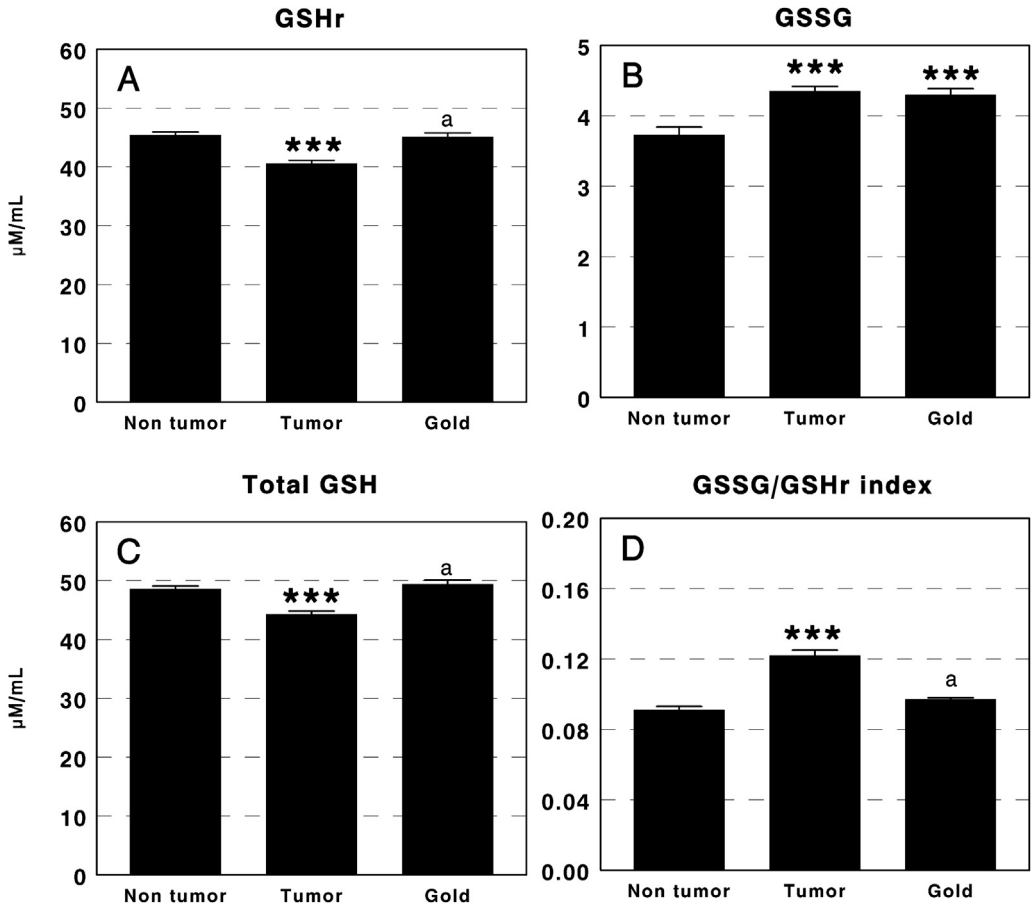

Fig. 7. A) Reduced glutathione (GSHr); B) oxidized glutathione (GSSG) and C) total glutathione (GSH) content and D) GSSG/GSHr index in serum of non-tumor healthy control animals treated with vehicle, and animals with C6 glioma implanted at the subcutaneous region treated with vehicle or with 20 μL of [Au(MANUH$_{-1}$)PPh$_3$] 6.5 mM during seven days. Results are expressed in μM/mL (Mean ± SEM; $n = 8$ animals per group; $^{***}P < 0.001$).

predispose the progression of cancer. Therefore, one of the mechanisms of action of the new compound [Au(MANUH$_{-1}$)PPh$_3$] could be potentiating antioxidant defense systems to avoid tumor growth and progression. Gromer et al. speculated that the C-terminal redox-active Cys-495/SeCys-49 center of the related enzyme thioredoxin reductase is the target of the gold(I) compounds as aurothioglucose and auranofin, whereas other selenium free enzymes such as glutathione reductase is far less sensitive to the inhibition of these compounds, but also inhibited GPx [59]. Ciftci et al. have showed that other gold(I) N-heterocyclic carbene complex also inhibits SOD, CAT and GPx activities in heart tissue [52]. However, the dose used in their work was much higher than the one used by us, which was also responsible of high levels of lipid peroxidation in heart tissue. Therefore, the repeated administration of very low doses of the title gold compound could be responsible of its effects on the enzyme and non-enzyme antioxidant defense systems and its relatively low adverse effects.

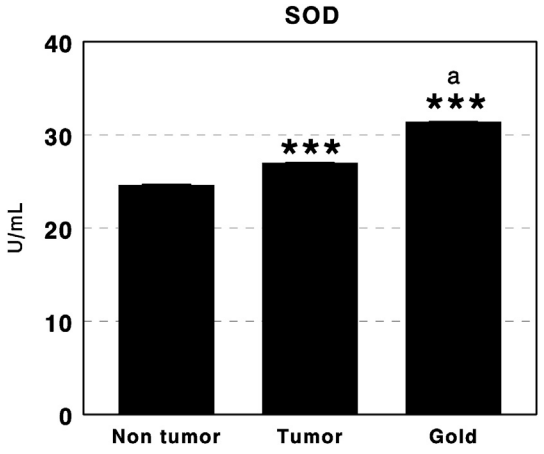

Fig. 8. Cu–Zn superoxide dismutase (SOD) activity in serum of non-tumor healthy control animals treated with vehicle, and animals with C6 glioma implanted at the subcutaneous region treated with vehicle or with 20 μL of [Au(MANUH$_{-1}$)PPh$_3$] 6.5 mM during seven days. Results are expressed in U/mL (Mean ± SEM; $n = 8$ animals per group; $^{***}P < 0.001$).

3.6. Effects of [Au(MANUH$_{-1}$)PPh$_3$] administration on blood serum chemistry

We have also measured some blood chemistry parameters (electrolytes, biomarkers of renal and hepatic functions and lipid profile) in order to analyze the potential adverse effects of [Au(MANUH$_{-1}$)PPh$_3$] treatment in several physiological processes.

No significant changes in the levels of calcium, phosphorus, sodium, potassium and chloride electrolytes have been observed in animals with and without glioma. After the treatment with [Au(MANUH$_{-1}$)PPh$_3$], the most altered parameter was the potassium level, which increases with respect to both healthy and tumoral animals (Table 3). This hyperkalemia must be due to the

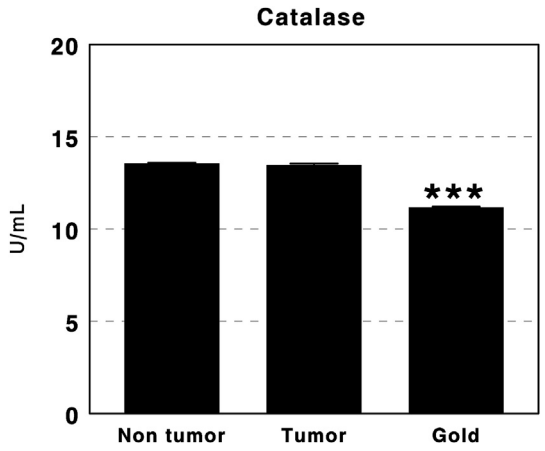

Fig. 9. Catalase (CAT) activity in serum of non-tumor healthy control animals treated with vehicle, and animals with C6 glioma implanted at the subcutaneous region treated with vehicle or with 20 μL of [Au(MANUH$_{-1}$)PPh$_3$] 6.5 mM during seven days. Results are expressed in U/mL (Mean ± SEM; $n = 8$ animals per group; $^{***}P < 0.001$).

death of tumor cells by gold(I) complex treatment. This tumor lysis syndrome typically follows administration of chemotherapy, and malignancies which have a large tumor burden, rapid turnover as well as speedy breakdown following chemotherapy are susceptible. However, its importance due to gold complex treatment is relatively low due to the non-variation observed in other electrolytes measured. Also, neither animals with tumors nor animals treated with [Au(MANUH$_{-1}$)PPh$_3$] showed significant differences in the levels of glucose, urea and creatinine when compared with the control group (see Table 4), but very high levels of uric acid were found as a consequence of tumor presence.

It has been hypothesized that the antioxidant properties of serum uric acid may play a crucial role in cancer etiology by preventing the formation of oxygen radicals, thereby protecting against carcinogenesis [60,61]. However several reports contain evidence contrary to the proposed antioxidant effect of serum uric acid against cancer, and instead indicate high levels to be independently associated with outcome, possibly reflecting a more serious prognostic indication [62]. In fact, it has been shown that astrocytoma patients' uric acid levels were significantly increased

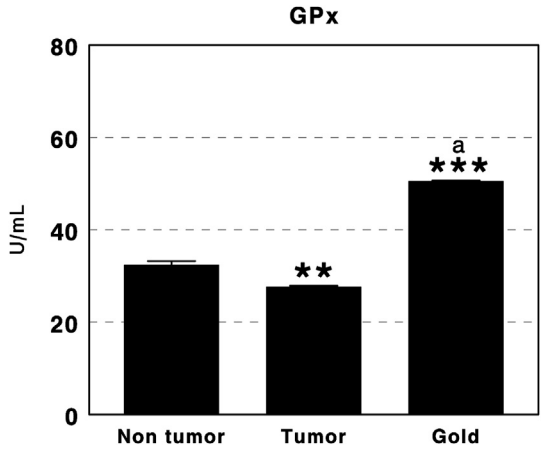

Fig. 10. Glutathione peroxidase (GPx) activity in serum of non-tumor healthy control animals treated with vehicle, and animals with C6 glioma implanted at the subcutaneous region treated with vehicle or with 20 μL of [Au(MANUH$_{-1}$)PPh$_3$] 6.5 mM during seven days. Results are expressed in U/mL (Mean ± SEM; $n = 8$ animals per group; $^{***}P < 0.001$).

Table 3
Serum levels of electrolytes in non-tumor animals (treated with vehicle only) and animals with C6 glioma implanted at the subcutaneous region treated with vehicle only or with [Au(MANUH$_{-1}$)PPh$_3$].

Parameter	Non-tumor group (vehicle)	Control tumor group (vehicle)	Treated tumor group (gold compound)	Significance level
Calcium (mg/dL)	10.4 ± 0.1	10.7 ± 0.2	10.3 ± 0.2	N.s.
Phosphorus (mg/dL)	8.3 ± 0.2	9.2 ± 0.6	8.3 ± 0.7	N.s
Sodium (mEq/L)	141.7 ± 0.9	143 ± 1	139.5 ± 0.6	N.s.
Potassium (mEq/L)	5.7 ± 0.1	5.7 ± 0.2	7.1 ± 0.5[a]	[a]$P < 0.001$
Chloride (mEq/L)	100.4 ± 0.9	100.0 ± 0.8	99.3 ± 0.5	N.s.

Data are expressed in the indicated units as mean ± SEM; $n = 8$ animals per group.
[a] Statistical significance.

in neoplastic compared with non-neoplastic tissue, and levels were even higher in necrotic tissue [63]. Therefore, our results agree with those reported by several authors [64,65]. However, after the treatment of glioma tumors with [Au(MANUH$_{-1}$)PPh$_3$] the levels of serum uric acid remained high. Therefore, the use of serum uric acid as biomarker of tumor progression needs further research.

Altered lipid profile patterns have been associated with malignancies because lipids play a pivotal role in the maintenance of cell integrity. Lower levels of serum cholesterol and other lipid constituents have been observed in patients with oral cancer, and it is thought to be due to their increased usage by tumor cells for new membrane biogenesis [66]. However, our results showed increased levels of total cholesterol, HDL-cholesterol and LDL-cholesterol in animals with glioma tumors treated with the vehicle or with [Au(MANUH$_{-1}$)PPh$_3$], this last group also showing increased the total cholesterol/HDL-cholesterol index (see Table 5). To our knowledge, no information is available on serum lipid profile with brain tumors, although cholesterol-lowering drugs are effective in inhibiting cancer cell proliferation [67]. Therefore, further research is necessary to better understand the underlying mechanisms of the regulation of serum cholesterol concentrations in cancer. In any case, the antitumor effects demonstrated by the new compound [Au(MANUH$_{-1}$)PPh$_3$] do not seem to be related to important changes in serum lipid profile.

Finally, in Table 6, serum levels of protein (total protein and albumin) and enzymes (alanine aminotransferase, aspartate aminotransferase and alkaline phosphatase) are given. Several authors have described increases in transaminases with cancer and cancer treatments. It is known that transaminases, such as aspartate aminotransferase and alanine aminotransferase, are intracellular enzymes that exist in only a small amount in the serum. Damage to liver cells may result in the leakage of enzymes into the plasma due to a high concentration gradient. Consequently, tumor related processes may lead to the release of this enzyme into the plasma as the result of autolytic breakdown or cellular necrosis. Also, the increase in the activities of these enzymes in the serum may result only consequent to impairment of the function of tissues

Table 4
Serum levels of glucose and non-protein nitrogenous compounds in non-tumor animals (treated with vehicle only) and animals with C6 glioma implanted at the subcutaneous region treated with vehicle only or with [Au(MANUH$_{-1}$)PPh$_3$].

Parameter	Non-tumor group (vehicle)	Control tumor group (vehicle)	Treated tumor group (gold compound)	Significance level
Glucose (mg/dL)	219 ± 12	221 ± 16	215 ± 16	N.s.
Urea (mg/dL)	41 ± 2	39 ± 2	41 ± 1	N.s.
Creatinine (mg/dL)	0.47 ± 0.02	0.5 ± 0.1	0.48 ± 0.03	N.s.
Uric acid ((mg/dL)	0.81 ± 0.04	1.2 ± 0.1[a]	1.6 ± 0.2[a]	[a]$P < 0.001$

Data are expressed in the indicated units as mean ± SEM; $n = 8$ animals per group.
[a] Statistical significance.

Table 5
Serum lipid profile in non-tumor animals (treated with vehicle only) and animals with C6 gliomas implanted at the subcutaneous region treated with vehicle only or with [Au(MANUH$_{-1}$)PPh$_3$].

Parameter	Non-tumor group (vehicle)	Control tumor group (vehicle)	Treated tumor group (gold compound)	Significance level
Total cholesterol (mg/dL)	60 ± 2	82 ± 5[a]	73 ± 1[a]	[a]$P < 0.001$
HDL-cholesterol (mg/dL)	30 ± 1	42 ± 4[a]	32 ± 2	[a]$P < 0.01$
LDL-cholesterol (mg/dL)	4 ± 1	11 ± 3[a]	13 ± 4[a]	[a]$P < 0.001$
Total cholesterol/ HDL-cholesterol	1.98 ± 0.03	2.0 ± 0.1	2.3 ± 0.1[a]	[a]$P < 0.01$
Triglycerides (mg/dL)	135 ± 13	155 ± 16	143 ± 12	N.s.

Data are expressed in the indicated units as mean ± SEM; $n = 8$ animals per group.
[a] Statistical significance.

with subsequent liberation of the enzymes into the circulation from the damaged tissue. In our glioma model, aspartate aminotransferase increased in both glioma animals treated with [Au(MANUH$_{-1}$)PPh$_3$] and vehicle only, indicating that this increase is exclusively due to the tumor process. However, animals treated with gold(I) compound also showed increased levels of alanine aminotransferase, indicating that this compound could induce certain liver damage. Future studies must determine if the increase in transaminases induced by [Au(MANUH$_{-1}$)PPh$_3$] is transient and reversible or not. However, the values found demonstrate only a 23% increase in alanine aminotransferase activity and do not seem to indicate irreversible, adverse effects on liver function in contrast with the antitumor efficacy of [Au(MANUH$_{-1}$)PPh$_3$] against malignant glioma. Similar results have been obtained with alkaline phosphatase that increased as a consequence of the tumor but not the treatment with the title compound. It has been recently described that alkaline phosphatase partly reflects osteoblastic activity, which is likely to be more pronounced in patients with larger volume or aggressive bony metastatic disease [68]. Serum alkaline phosphatase is a relatively nonspecific biomarker and can be elevated from sources other than bone (e.g., the liver). Patients with bone metastases and elevated baseline alkaline phosphatase are likely to have bone as the dominant source of the enzyme, and are likely to have liver metastases that cause alkaline phosphatase elevations. In any case, we have not detected in our model the presence of metastases, although the presence of micrometastases in several other organs/tissues including liver could explain the increase in this enzyme activity.

Table 6
Serum levels of proteins and enzymes in non-tumor animals (treated with vehicle only) and animals with C6 gliomas implanted at the subcutaneous region treated with vehicle only or with [Au(MANUH$_{-1}$)PPh$_3$].

Parameter	Non-tumor group (vehicle)	Control tumor group (vehicle)	Treated tumor group (gold compound)	Significance level
Total protein (mg/mL)	59.0 ± 0.1	57.0 ± 0.1	55.5 ± 0.1	N.s.
Albumin (g/dL)	2.88 ± 0.03	2.95 ± 0.04	2.85 ± 0.09	N.s.
Alanine aminotransferase (UI/L)	49 ± 6	44 ± 2	60 ± 5[a]	[a]$P < 0.001$
Aspartate aminotransferase (UI/L)	146 ± 11	240 ± 24[a]	249 ± 81[a]	[a]$P < 0.001$
Alkalin phosphatase (UI/L)	105 ± 10	157 ± 15[a]	158 ± 8[a]	[a]$P < 0.001$

Data are expressed in the indicated units as mean ± SEM; $n = 8$ animals per group.
[a] Statistical significance.

Therefore, we conclude that the treatment with [Au(MANUH$_{-1}$)PPh$_3$] during short time periods against glioma tumors effectively inhibited tumor growth through mechanisms that involved endogenous enzymatic and non-enzymatic antioxidant defenses, as demonstrated by the decrease in the oxidative stress biomarkers TBARS and protein oxidation levels. Thus, the treatment with [Au(MANUH$_{-1}$)PPh$_3$] maintains the non-enzyme antioxidant defense systems as in healthy animals, and modifies positively the enzyme antioxidant defense systems. Finally, the used of this complex yields few adverse effects related to liver damage to some extent.

4. Experimental

4.1. Chemistry

4.1.1. Apparatus

C, H, N microanalyses were performed on a Thermofinnigan Flash 1112 Series elemental analyzer. IR spectra were measured on Bruker FT-IR Tensor-27 (4000–400 cm^{-1}, KBr pellets) and Vector-22 (600–220 cm^{-1}, polyethylene pellets) spectrophotometers. UV–Vis spectrum (900–250 nm, 5×10^{-5} M DMSO:H_2O 1:1 solution) was recorded on a Varian Cary 4000 UV–Vis spectrophotometer. NMR spectra (^{1}H, ^{13}C and ^{31}P) were recorded using a Bruker Avance 400 MHz apparatus (DMSO-d_6 solutions, δ(TMS) = 0.0 ppm). ^{13}C CP/MASS NMR spectra of solid samples were measured in a Bruker Avance 500 MHz with TOSS pulse sequence to eliminate spinning side bands. Electron impact (EI) MS spectrum was recorded on a Thermo DSQ-II spectrometer. Chemicals were purchased from ABCR and Alfa-Aesar and used without further purification.

4.1.2. Synthesis of (6-amino-1-methyl-5-nitrosouracilato-N3)-triphenylphosphinegold(I)

The uracil derivative was prepared following an established procedure [14]. The gold(I) complex was prepared as follows: A solution of [AuCl(PPh$_3$)] (0.0625 mmol in 10 mL of acetone) was added to a solution of the pyrimidine derivative (0.25 mmol in 20 mL CH_3OH) containing 0.25 mmol of KOH. The resulting solution was heated for 3 h. It was left to cool to room temperature and, after several days, crystals suitable for X-ray diffraction were obtained. Yield: *ca.* 20%. $AuC_{23}H_{20.5}N_4O_{3.25}P$; $M = 632.91$ g/mol; Anal. Found (%): C, 43.76; H, 3.23; N, 8.95; Calc. (%) C, 43.64; H, 3.27; N, 8.85. MS(EI): 629 [M$^+$], 459 [M$^+$ − MANU], 262 [M$^+$ − (Au–MANU)]. UV–vis (λ nm, ε l mol^{-1} cm^{-1}): 523, 2.3×10^3; 320, 16.4×10^3. IR (KBr, cm^{-1}): 3443, 3052, 1681, 1615, 1525, 1437, 1482, 1176, 1136, 1102, 694, 511, 506. ^{1}H NMR (DMSO-d_6): δ 3.23 (s, 3H, N1–CH_3), 7.66–7.60 (m, 15H, C_6H_5) 8.8 (s, 1H, N6–H), 13.28 (s, 1H, N6–H). ^{13}C NMR (DMSO-d_6): δ 133.78 (d, $J = 17.05$, 2C), 132.29 (s, CH), 129.60 (d, $J = 18.95$, 2C) and 128.26 ppm (s, C) (only triphenylphosphine signals were observed). ^{13}C NMR CPTOSS (solid): δ 28.86, 29.90 (s, C1), 155.98, 154.72 (s, C2), 167.60 (s, C4), 141.29 (s, C5), 150.01 (s, C6), 129.79 (broad signal, PPh_3). ^{31}P{^{1}H} NMR (161.9 MHz, DMSO-d_6): δ 31.38 ppm.

4.1.3. X-ray crystallography

X-ray crystal structure data for [Au(MANUH$_{-1}$)PPh$_3$]·¼H_2O. CCDC number 868875: $C_{92}H_{80}Au_4N_{16}O_{13}P_4$; $M = 2529.48$; Orthorhombic, Pbna; unit cell $a = 17.898(4)$, $b = 22.491(2)$, $c = 23.400(5)$ Å; $V = 9420.3(3)$ Å^3; $T = 120(2)$ K; Bruker–Nonius KappaCCD apparatus, graphite-monochromated Mo-Kα radiation ($\lambda = 0.71073$ Å); $Z = 4$; $D_x = 1.784$ Mg m^{-3}; $F(000) = 4896$; pink prismatic (0.22 × 0.14

$\times$ 0.10 mm^3); μ = 6.348 mm^{-1}; θ = 2.5–27.5°, $-23 < h < 18$, $-27 < k < 29$, $-30 < l < 30$; 108,509 measured reflections, 10,817 independent (R_{int} = 0.092), 7814 with $I > 2\sigma(I)$ used in the refinement. Lorentz, polarization and multi-scan absorption corrections were applied with SADABS [69], min. and max. transmission were 0.3357 and 0.5693. Weighting scheme $w^{-1} = \sigma^2(F_o^2) + (0.0126P)^2 + 62.7198P$, where $P = 1/3(F_o^2 + 2F_c^2)$. Final R and wR [$I > 2\sigma(I)$] were 0.0495 and 0.0735, data-to-parameter ratio 18.2, goodness-of-fit on F^2 = 1.079, largest diff. peak and hole in the Fourier map were 1.484 and −1.260 e Å^{-3}.

The structure was solved by direct methods and refined using SHELXL97 program [70] inside the WinGX package [71] employing full-matrix least-squares methods on F^2. All non-H atoms were refined anisotropically; all hydrogen atoms were placed in calculated positions following riding models except those of the amino group in 6′ position, which were found in subsequent difference maps and isotropically refined. All calculations and graphics were carried out with PLATON [72] and MERCURY [73].

4.1.4. Computational details

The calculations conducted in this research were performed with the suite of programs Gaussian09 [74]. Likewise, the topological analysis of the wavefunctions was accomplished within Bader's Atoms in Molecules theory [34], i.e., the interactions among the different atoms were characterized through the parameters defining the Bond Critical Points (BCPs) appearing between them. The results were obtained with the program AIM2000 [75,76].

After proper calibration (please, see Supplementary information) of different approaches of the WFT and DFT types using as reference CCSD(T) [77], the Scuseria et al.'s TPSS exchange functional combined with their τ-dependent gradient-corrected functional, TPSS [78] was chosen. In addition, Hirao et al.'s corrections for the long range term [79] were applied to the TPSSTPSS functional yielding the method LC-TPSSTPSS. For the basis sets, the 3-ζ Atomic Natural Orbital (ANO-RCC) basis set [80,81] was used on the gold atoms to produce the wavefunctions of the binuclear complex. For the other atoms, Dunning aug-cc-pVTZ and aug-cc-pVDZ were used on the nitrogen atom linked to Au, aug-cc-pVTZ on P atom and Pople 6-31++G(d,p) on the remaining ones.

The calculations of the wavefunctions with an all electron basis sets were done by using the second order scalar Douglas–Kress–Hall's approximation (*integral = dkh*) [82,83]. More information about computational details is supplied in Supplementary material.

4.2. Biology

4.2.1. Cell culture

C6 glioma cells were grown in 5% fetal bovine serum (FBS)-supplemented DMEM/HAM F-12 medium without antibiotics. Cells were incubated at 37 °C in a modified atmosphere of 5% CO_2/95% air until reaching confluence. Freedom from mycoplasma contamination was checked regularly by testing with Hoechst 33528.

4.2.2. Colorimetric cytotoxic assay

To set up the colorimetric cytotoxic assay (CCA) cells were trypsinized from monolayer and diluted to 4 $\times$ 10^4 cells/mL. Cells were in exponential phase of growth during the whole experiment. Aliquots of 1 mL of cells were pipetted into wells of 24-well tissue culture plates (Nunc) and the plates were incubated for 24 h. The gold compound [Au(MANUH$_{-1}$)PPh$_3$] was then added to the wells in a volume of 1 mL per well at a range of concentrations (2, 4, 6, 8 and 10 μM), each dose being used in at least four replicate wells. After 3 days incubation, the medium was removed and the cultures were washed with PBS prior to fixation with 10% trichloroacetic acid (TCA) for 30 min. After, the cultures were washed with tap water to remove TCA. Plates were air dried and then stored until use. TCA-fixed cells were stained for 20 min with 0.4% (w/v) sulforhodamine B (SRB) (Sigma) dissolved in 1% acetic acid. At the end of staining period, SRB was removed and cultures were rinsed with 1% acetic acid to remove unbound dye. The cultures were air dried and bound dye was solubilized with 10 mM Tris base (pH 10.5). Optical density (OD) was read in a Tecan Genios Plus plate reader at 492 nm. The photometer response was linear with dye concentration and it was proportional to cell numbers counted in parallel with an automated cell counter (TC10, BioRad). The values of fraction of cell growth affected (Fa) by drug dosage were used to compute the values of the dose required for 50% inhibition of cell growth or IC50 (Dm), the coefficient of the sigmoidicity of the dose–effect curve (m) and the linear correlation coefficient of the median–effect plot (r).

4.2.3. Animals and treatments

Twenty-four male Wistar rats (264 ± 3.2 g body weight) were used in this study. The animals were provided from the animal house-care of the University of Jaen, and maintained in an environment controlled under constant temperature (25 °C) with a 12 h-light/12 h-dark cycle. Rats were housed in cages and given free access to standard laboratory rat food and water. The experimental procedures for animal use and care were in accordance with the European Community Council directive (86/609/EEC). Protocols were approved by the Bioethical Committee of the University of Jaen. Animals were randomly divided into three groups of eight rats each. Two groups were used for the implantation of C6 glioma cells (tumor groups), whereas one group remained as non-tumor, healthy control group. Ten days after C6 glioma cell implantation, one of the tumor groups was injected subcutaneously daily with 20 μL of [Au(MANUH$_{-1}$)PPh$_3$] 6.5 mM (0.15 mg/kg body weight) dissolved in 50% dimethylsulfoxide (DMSO) for seven days. The other tumor group and the non-tumor group received vehicle-only injections (50% DMSO) for the same time period.

4.2.4. Implantation of C6 glioma cells

Five million C6 glioma cells suspended in 50 μL of culture medium without FBS were injected subcutaneously in both dorsal flanks of the rats using a Hamilton syringe with a 26-gauge needle. The same procedure without cells was performed in the non-tumor group.

4.2.5. Measurement of tumor volume and collection of the tissue and serum

The size of the abdominal tumor was measured with slide calipers ten days after C6 glioma cells implantation just before the beginning of the treatments and after seven days of treatment. The tumor volume was defined as ½(ab)^2 (a: long diameter, b: short diameter) [53]. Rats were anesthetized with equitensin (2 mL/kg body weight) by intraperitoneal injection and then shaved and sterilized with 10% povidone–iodine. Samples of tumors were quickly removed and prepared for histopathological examination. Blood samples were also obtained through the left cardiac ventricle, drawn into tubes without anticoagulant, allowed to clot, and then centrifuged for 10 min at 3000 g to obtain the serum, which was frozen and stored at −80 °C until use.

4.2.6. Histopathological examination

The resective tumors were treated with formalin and the specimens were dehydrated and embedded in paraffin. The sections were stained by hematoxylin and eosin (H&E). Microphotography was performed using a Nikon NIS-Elements F V.3.2 imaging system.

4.2.7. Oxidative stress parameters assays

4.2.7.1. Lipid peroxidation assay. Lipid peroxidation was measured by analyzing the amount of thiobarbituric acid reactive substances (TBARS) as previously described [84]. Briefly, 25 μL of each sample was mixed with 100 μL of ice-cold 20% trichloroacetic acid (TCA). After centrifugation, a volume of supernatant was added to an equal volume of 0.67% 4,6-dihydroxypyrimidine-2-thiol (TBA) and the mixture was kept in a boiling water bath for 15 min. Samples were cooled to room temperature and the absorbance at 532 nm was recorded after subtracting blanks containing TCA and TBA in an equal volume. The signal was read against a malondialdehyde (MDA) standard curve and the results were expressed as mg/mL.

4.2.7.2. Protein oxidation assay. The protein contents of the carbonyl groups were determined as previously described [84]. Briefly, 25 μL of sample was mixed with 100 μL of ice-cold 20% TCA and centrifuged. Protein precipitates were left to react with 2,4-dinitrophenylhydrazine 10 mM for an hour at room temperature in the dark. After the reaction, proteins were precipitated with 20% TCA and unreacted dye was washed twice with 10% TCA. The pellets were dissolved in 1 M NaOH and absorbances were recorded at 360 nm. The results were expressed as nmol per mg of protein using an extinction coefficient of $2.0 \times 10^4\ M^{-1}\ cm^{-1}$.

4.2.7.3. Determination of glutathione (GSH) and glutathione disulfide (GSSG). GSH levels were measured as described by Griffith with minor modifications [85]. For this purpose, serum samples were treated with two volumes of buffer, centrifugated at 10,000 *g* for 5 min at 4 °C and the pellet discarded. Supernatants containing total GSH were mixed with 0.6 mg/mL of 5,5-dithiobis(2-nitrobenzoic acid) (DTNB) and 0.248 mg/mL nicotinamide adenine dinucleotide phosphate (NADPH). The reaction was started on addition of 1 U/mL GSSG reductase. Absorbance was measured at 405 nm at 30 °C in a TECAN GENios Plus spectrophotometer every 20 s for 2 min. For GSSG determination, 2-vinylpyridine was used to derivatize GSH. Data are presented as nmol of total GSH (GSH plus GSSG) per mg of total protein.

4.2.7.4. Catalase activity assay. Plasma samples were processed and analyzed for catalase (E.C.: 1.11.1.6) activity as described by Aebi [86] with slight modifications by Cohen [87].

4.2.7.5. Superoxide dismutase assay. SOD activity was as measured according to Paoletti [88]. Ten microliters of protein solution was mixed with reaction buffer contained 100 mM, TDB buffer (triethanolamide–diethanolamide, pH 7.4), 7.5 mM NADH and relation 1:2 EDTA/$MnCl_2$. To start the reaction, 25 μL of 10 mM mercaptoethanol was added. The absorbance at 340 nm between 2 and 15 min was recorded.

4.2.7.6. Glutathione peroxidase activity assay. GPx activity was measured according to Ellerby and Bredesen [89]. The reaction mixture was formed by 50 mM potassium phosphate (pH 7.4) 25 mM NADPH, 1 mmol/L of GSH, 100 U/mL of yeast GRd. Ten microliters of protein solution per sample were added and mixed with the reaction mixture in a 96-well dish. The hydroperoxide-independent NADPH consumption rate was recorded for 3 min at 37 °C at 340 nm in an automatic microplate reader (TECAN GENios Plus). Then, 2.5 μL of tert-butylhydroperoxide was added to start the reaction, mixed, and the overall rate at 340 nm was recorded. The same procedure was carried out in the same reaction volume without the sample protein. This allows subtracting from the total rate, the non-enzymatic rate of GSH oxidation.

4.2.8. Blood serum chemistry measurements

Electrolytes (sodium, potassium and chloride) were assayed using selective ion electrodes, according to Shibata [90]. Results are expressed in mEq/L; calcium was assayed by colorimetric assay, according to Farrell [91], and phosphorus was assayed by colorimetric assay, according to Tietz [92]. Results are expressed in mg/dL. The non-protein nitrogenous compounds uric acid, urea, creatinine, and glucose in serum samples were assessed using commercial kits (Boehringer Mannheim) with the automated Roche-Hitachi 917 system, according to the methods described by Praetorius and Poulsen [93], Talke and Schubert [94], Bartels [95] and Peterson and Young [96], respectively. Total cholesterol, high-density lipoprotein (HDL) cholesterol and triglycerides were assayed with the use of standard enzymatic colorimetric methods using commercially available kits according to Roeschlau [97], Sugiuchi [98] and Siedel [99]. The low-density lipoprotein (LDL) cholesterol level was calculated according to the Friedewald formula. Results are expressed in mg/mL. Serum activities of aspartate aminotransferase (AST) and alanine aminotransferase (ALT) were estimated by quantitative enzymatic colorimetric, end point methods using commercially available kits according to Tietz [92] and Bergmeyer [100]. Results are expressed in UI/L. The serum alkaline phosphatase (ALP) was determined by colorimetric, end point method using commercially available kits, according to Belfield and Goldberg [101]. Results are expressed in UI/L. The serum albumin content was determined by colorimetric method using a commercial kit according to Doumas [102]. Results are expressed in g/dL. The serum total protein was estimated by the colorimetric method of Bradford [103]. Results are expressed in mg/mL.

4.2.9. Statistical analysis

All values represent the mean ± standard error of the mean (SEM). Data were analyzed by ANOVA plus Newman–Keuls test, using IBM SPSS V.19 software. Values of $P < 0.05$ were considered significant.

5. Conclusions

A new linear N–Au^{I}–P complex containing the 6-amino-1-methyl-5-nitrosouracilato-N^3 anion and triphenylphosphine was prepared, structurally characterized and biologically investigated in an animal model of experimental glioma. After seven days of treatment the tumor growth was significantly reduced and the oxidative stress parameters decreased to values similar to non-tumor healthy control animals. Also, the non-enzyme antioxidant defense systems are maintained and enzyme antioxidant defenses are increased. The analysis of blood serum parameters indicates few adverse effects.

Acknowledgments

The study was supported by the Universidad de Jaén (Plan de Apoyo a la Investigación, al Desarrollo Tecnológico y a la Innovación), Junta de Andalucía (PAIDI groups FQM273, FQM337 and BIO296 and Proyecto de Excelencia Motriz CVI2009-4957M) and Instituto de Estudios Giennenses (grant IEG-2009). Thanks are due to Dr. M.I. Torres for anatomopathological studies. Computational resources supplied by the Centro de Servicios de Informática y Redes de Comunicaciones (CSIRC-University of Granada, Spain) and the Centro Informático Científico de Andalucía (CICA, Spain) are also acknowledged.

Appendix A. Supplementary data

Supplementary data related to this article can be found at http://dx.doi.org/10.1016/j.ejmech.2013.03.067. These data include MOL

files and InChiKeys of the most important compounds described in this article.

References

[1] M.L. Bondy, M.E. Scheurer, B. Malmer, J.S. Barnholtz-Sloan, F.G. Davis, D. Il'yasova, C. Kruchko, B.J. McCarthy, P. Rajaraman, J.A. Schwartzbaum, S. Sadetzki, B. Schlehofer, T. Tihan, J.L. Wiemels, M. Wrensch, P.A. Buffler, Cancer 113 (2008) 1953–1968.
[2] F.G. Davis, B.S. Malmer, K. Aldape, J.S. Barnholtz-Sloan, M.L. Bondy, T. Brannstrom, J.M. Bruner, P.C. Burger, V.P. Collins, P.D. Inskip, C. Kruchko, B.J. McCarthy, R.E. McLendon, S. Sadetzki, T. Tihan, M.R. Wrensch, P.A. Buffler, Cancer Epidemiol. Biomarkers Prev. 17 (2008) 484–489.
[3] P. Rajaraman, A. Hutchinson, N. Rothman, P.M. Black, H.A. Fine, J.S. Loeffler, R.G. Selker, W.R. Shapiro, M.S. Linet, P.D. Inskip, Neuro Oncol. 10 (2008) 709–715.
[4] T. Papacocea, R. Papacocea, A. Badarau, A.D. Ion, I. Buraga, L. Gaman, A. Papacocea, Ther. Pharmacol. Clin. Toxicol. XV (2011) 234–239.
[5] P. Benda, J. Lightbody, G. Sato, L. Levine, W. Sweet, Science 161 (1968) 370–371.
[6] D.L. Peterson, P.J. Sheridan, W.E. Brown Jr., J. Neurosurg. 80 (1994) 865–876.
[7] A.T. Parsa, I. Chakrabarti, P.T. Hurley, J.H. Chi, J.S. Hall, M.G. Kaiser, J.N. Bruce, Neurosurgery 47 (2000) 993–999. (Discussion 999–1000).
[8] K. Watanabe, M. Sakamoto, M. Somiya, M.R. Amin, H. Kamitani, T. Watanabe, Neurol. Res. 24 (2002) 485–490.
[9] I. Ott, Coord. Chem. Rev. 253 (2009) 1670–1681.
[10] A. Bindoli, M.P. Rigobello, G. Scutari, C. Cabbiani, A. Casini, L. Mesori, Coord. Chem. Rev. 253 (2009) 1692–1707.
[11] S.P. Fricker, Anti-Cancer Agents Med. Chem. 11 (2011) 940–952.
[12] D. Krishnamurthy, M.R. Karver, E. Fiorillo, V. Orru, S.M. Stanford, N. Bottini, A.M. Barrios, J. Med. Chem. 51 (2008) 4790–4795.
[13] X. Zhang, M. Frezza, V. Milacic, L. Ronconi, Y.H. Fan, C.F. Bi, D. Fregona, Q.P. Dou, J. Cell. Biochem. 109 (2010) 162–172.
[14] Y. Nagayama, S. Harakawa, A. Taguchi, A. Takashita, K. Eguchi, N. Yokoyama, S. Nataki, Horm. Metab. Res. 25 (1993) 657–658.
[15] F. Mendes, M. Groessl, A.A. Nazarov, Y.O. Tsybin, G. Sava, I. Santos, P.J. Dyson, A. Casini, J. Med. Chem. 54 (2011) 2196–2206.
[16] S. Tian, F.M. Siu, S.C.F. Kui, C.N. Lok, C.M. Che, Chem. Commun. 47 (2011) 9318–9320.
[17] C.M. Che, R.W.Y. Sun, Chem. Commun. 47 (2011) 9554–9560.
[18] J.C. Lima, L. Rodríguez, Anti-Cancer Agents Med. Chem. 11 (2011) 921–928.
[19] N.A. Illán Cabeza, R.A. Vilaplana, Y. Alvarez, K. Akdi, S. Kamah, F. Hueso Ureña, M. Quirós, F. González Vílchez, M.N. Moreno Carretero, J. Biol. Inorg. Chem. 10 (2005) 924–934.
[20] N.A. Illán Cabeza, S.B. Jiménez Pulido, M.N. Moreno Carretero, J.M. Martínez Martos, M.J. Ramírez-Expósito, J. Inorg. Biochem. 103 (2009) 1176–1184.
[21] N.A. Illán-Cabeza, A.R. García-García, M.N. Moreno-Carretero, J.M. Martínez-Martos, M.J. Ramírez-Expósito, J. Inorg. Biochem. 99 (2005) 1637–1645.
[22] K. Nakamoto (Ed.), Infrared and Raman Spectra of Inorganic and Coordination Compounds, Wiley & Sons, New York, 1997.
[23] W.T. Dixon, J. Schafer, M.D. Sefcik, E.O. Stejskal, R.A. McKay, J. Magn. Reson. 49 (1982) 341–345.
[24] K. Nomiya, R. Noguchi, K. Ohsawa, K. Tsuda, J. Chem. Soc. Dalton Trans. (1998) 4101–4108.
[25] L. Rodríguez, C. Lodeiro, J.C. Lima, R. Crehuet, Inorg. Chem. 47 (2008) 4952–4962.
[26] E. Colacio, R. Cuesta, J.M. Gutiérrez-Zorrilla, A. Luque, P. Román, T. Giraldi, M.R. Taylor, Inorg. Chem. 35 (1996) 4232–4238.
[27] K. Nomiya, R. Noguchi, K. Ohsawa, K. Tsuda, M. Oda, J. Inorg. Biochem. 78 (2000) 363–370.
[28] K. Nomiya, R. Noguchi, M. Oda, Inorg. Chim. Acta 298 (2000) 24–32.
[29] B. Lippert, G. Neugebauer, Inorg. Chim. Acta 46 (1980) 171–179.
[30] G. Kampf, M. Willermann, E. Freisinger, B. Lippert, Inorg. Chim. Acta 330 (2002) 179–188.
[31] P.J. Sanz-Miguel, P. Lax, M. Willermann, B. Lippert, Inorg. Chim. Acta 357 (2004) 4552–4561.
[32] N.A. Illán-Cabeza, A.R. García-García, M.N. Moreno-Carretero, Comput. Theor. Chem. 964 (2011) 83–90.
[33] C.J. Janiak, Dalton Trans. (2000) 3885–3896.
[34] R.F.W. Bader, Atoms in Molecules: A Quantum Theory, Clarendon Press, Oxford, England, 1990.
[35] A. Federico, F. Morgillo, C. Tuccillo, F. Ciardiello, C. Loguercio, Int. J. Cancer 121 (2007) 2381–2386.
[36] U. Nair, H. Bartsch, J. Nair, Free Radic. Biol. Med. 43 (2007) 1109–1120.
[37] B. Halliwell, J.M.C. Gutteridge (Eds.), Free Radicals in Biology and Medicine, third ed., Oxford Science Pub., UK, 1999.
[38] S.S. Khanzode, M.G. Muddeshwar, S.D. Khanzode, G.N. Dakhale, Free Radic. Res. 38 (2004) 81–85.
[39] A. Gonenc, Y. Ozkan, M. Torun, B. Simsek, J. Clin. Pharm. Ther. 26 (2001) 141–144.
[40] T.W. Kwon, B.M. Watss, J. Food Sci. 29 (1964) 294–302.
[41] Y. Zhang, S.Y. Chen, T. Hsu, R.M. Santella, Carcinogenesis 23 (2002) 207–211.
[42] G.M. Rao, A.V. Rao, A. Raja, S. Rao, A. Rao, Clin. Chim. Acta 296 (2000) 203–212.
[43] R.A. Floyd, FASEB J. 4 (1990) 2587–2597.
[44] G. Ray, S. Batra, N.K. Shukla, S. Deo, V. Raina, S. Ashok, S.A. Husain, Breast Cancer Res. Treat. 59 (2000) 163–170.
[45] A. Geetha, S. Karthiga, G. Surendran, G. Jayalakshmi, J. Lab. Med. 2 (2001) 20–27.
[46] K. Kolanjiappan, S. Manoharan, M. Kayalvizhi, Clin. Chim. Acta 326 (2002) 143–149.
[47] E. Zengin, P. Atukeren, E. Kokoglu, M.K. Gumustas, U. Zengin, Clin. Neurol. Neurosurg. 111 (2009) 345–351.
[48] D.F. Louw, R. Bose, A.A. Sima, G.R. Sutherland, Neurosurgery 41 (1997) 1146–1150. (Discussion 1151).
[49] F. Lamari, R. La Schiazza, R. Guillevin, B. Hainque, M.J. Foglietti, J.L. Beaudeux, M. Bernard, Ann. Biol. Clin. Paris 66 (2008) 143–150.
[50] B. Cirak, S. Inci, S. Palaoglu, V. Bertan, Clin. Chim. Acta 327 (2003) 103–107.
[51] J. Guo, L. Prokai, J. Proteomics 74 (2011) 2360–2369.
[52] O. Ciftci, I. Ozdemir, O. Cakir, S. Demir, Toxicol. Ind. Health 27 (8) (2011) 735–741.
[53] J. Navarro, E. Obrador, J. Carretero, I. Petschen, J. Avino, P. Perez, J.M. Estrela, Free Radic. Biol. Med. 26 (1999) 410–418.
[54] B. Popov, V. Gadjeva, P. Valkanov, S. Popova, A. Tolekova, Arch. Physiol. Biochem. 111 (2003) 455–459.
[55] S. Aggarwal, M. Subberwal, S. Kumar, M.J. Sharma, Cancer Res. Ther. 2 (2006) 24–27.
[56] R.F. Del Maestro, W. McDonald, R. Anderson, in: R. Greenwald, G. Cohen (Eds.), Oxy Radicals and Their Scavenger Systems, Elsevier, New York, 1983, pp. 28–35.
[57] N. Yilmaz, H. Dulger, N. Kiymaz, C. Yilmaz, I. Bayram, B. Ragip, M. Oger, Int. J. Neurosci. 116 (2006) 937–943.
[58] A.S. Gauchez, J. Riondel, M. Jacrot, J. Calop, A. Favier, Biol. Trace Elem. Res. 47 (1995) 103–109.
[59] S. Gromer, L.D. Arscott, C.H. Williams, R.H. Schirmer, K. Becker, J. Biol. Chem. 273 (1998) 20096–20101.
[60] I. Fridovich, Ann. N. Y. Acad. Sci. 893 (1999) 13–18.
[61] D.J. Betteridge, Metabolism 49 (2000) 3–8.
[62] A.M. Strasak, K. Rapp, W. Hilbe, W. Oberaigner, E. Ruttmann, H. Concin, G. Diem, K.P. Pfeiffer, H. Ulmer, Ann. Oncol. 18 (2007) 1893–1897.
[63] H. Landolt, H. Langemann, A. Probst, O. Gratzl, J. Neurooncol. 21 (1994) 127–133.
[64] T. Ueda, S. Wakisaka, K. Kinoshita, H. Adachi, No To Shinkei 36 (1984) 255–260.
[65] S. Pietila, A. Makipernaa, H. Sievanen, A.M. Koivisto, T. Wigren, H.L. Lenko, Pediatr. Blood Cancer 52 (2009) 853–859.
[66] G. Ghosh, K.M. Jayaram, R.V. Patil, S. Malik, J. Contemp. Dent. Pract. 12 (2011) 451–456.
[67] G. Fagherazzi, A. Fabre, M.C. Boutron-Ruault, F. Clavel-Chapelon, Eur. J. Cancer Prev. 19 (2010) 120–125.
[68] G. Sonpavde, G.R. Pond, W.R. Berry, R. de Wit, A.J. Armstrong, M.A. Eisenberger, I.F. Tannock, Urol. Oncol. 30 (2012) 607–613.
[69] G.M. Sheldrick, SADABS 2.10 (2003).
[70] G.M. Sheldrick, SHELXL-97, University of Göttingen, Germany, 1997.
[71] L.J. Farrugia, WINGX 1.70.01, University of Glasgow, Scotland, 2005.
[72] A.L. Spek, PLATON A Multipurpose Crystallographic Tool, Utrecht University, Utrecht, The Netherlands, 2003.
[73] MERCURY 3.0.1, Cambridge Crystallographic Data Centre, Cambridge, England, 2002.
[74] M.J. Frisch, G.W. Trucks, H.B. Schlegel, G.E. Scuseria, M.A. Robb, J.R. Cheeseman, G. Scalmani, V. Barone, B. Mennucci, G.A. Petersson, H. Nakatsuji, M. Caricato, X. Li, H.P. Hratchian, A.F. Izmaylov, J. Bloino, G. Zheng, J.L. Sonnenberg, M. Hada, M. Ehara, K. Toyota, R. Fukuda, J. Hasegawa, M. Ishida, T. Nakajima, Y. Honda, O. Kitao, H. Nakai, T. Vreven, J.A. Montgomery Jr., J.E. Peralta, F. Ogliaro, M. Bearpark, J.J. Heyd, E. Brothers, K.N. Kudin, V.N. Staroverov, T. Keith, R. Kobayashi, J. Normand, K. Raghavachari, A. Rendell, J.C. Burant, S.S. Iyengar, J. Tomasi, M. Cossi, N. Rega, J.M. Millam, M. Klene, J.E. Knox, J.B. Cross, V. Bakken, C. Adamo, J. Jaramillo, R. Gomperts, R. Stratmann, O. Yazyev, A.J. Austin, R. Cammi, C. Pomelli, J.W. Ochterski, R.L. Martin, K. Morokuma, V.G. Zakrzewski, G.A. Voth, P. Salvador, J.J. Dannenberg, S. Dapprich, A.D. Daniels, Ö. Farkas, J.B. Foresman, J.V. Ortiz, J. Cioslowski, D.J. Fox, Gaussian 09, Revision B.01, Gaussian Inc., Wallingford, CT, 2010.
[75] F. Biegler-König, J. Schönbohm, D. Bayles, J. Comput. Chem. 22 (2001) 545–559.
[76] F. Biegler-König, J. Schönbohm, J. Comput. Chem. 23 (2002) 1489–1494.
[77] J.A. Pople, M. Head-Gordon, K. Raghavachari, J. Chem. Phys. 87 (1987) 5968–5975.
[78] J.M. Tao, J.P. Perdew, V.N. Staroverov, G.E. Scuseria, Phys. Rev. Lett. 91 (2003) 146401.
[79] H. Iikura, T. Tsuneda, T. Yanai, K.J. Hirao, Chem. Phys. 115 (2001) 3540–3544.
[80] B.O. Roos, R. Lindh, P.A. Malmqvist, V. Veryazov, P.O. Widmark, J. Phys. Chem. A 108 (2004) 2851–2858.
[81] B.O. Roos, R. Lindh, P.A. Malmqvist, V. Veryazov, P.O. Widmark, J. Phys. Chem. A 109 (2005) 6575–6579.
[82] M. Douglas, N.M. Kroll, Ann. Phys. 82 (1974) 89–155.
[83] B.A. Hess, P. Chandra, Phys. Scr. 36 (1987) 412–415.
[84] M.D. Mayas, M.J. Ramírez-Expósito, M.J. García, M.P. Carrera, J.M. Martínez Martos, Alcohol 46 (2012) 481–487.
[85] O.W. Griffith, Anal. Biochem. 106 (1980) 207–212.

[86] H. Aebi, Methods Enzymol. 105 (1984) 121–126.
[87] G. Cohen, M. Kim, V. Ogwu, J. Neurosci. Methods 67 (1996) 53–56.
[88] F. Paoletti, D. Aldinucci, A. Mocali, A. Caparrini, Anal. Biochem. 154 (1986) 536–541.
[89] L.M. Ellerby, D.E. Bredesen, Methods Enzymol. 322 (2000) 413–421.
[90] Y. Shibata, T. Maruizume, H. Miyage, J. Chem. Soc. Jpn. 9 (1992) 961–967.
[91] E.C. Farrell, in: A.J. Pesce, L.A. Kaplan (Eds.), Calcium, Methods in Clinical Chemistry, Mosby, 1987, pp. 865–869.
[92] N.W. Tietz, Clinical Guide to Laboratory Tests, Saunders Company, Philadelphia, 1995.
[93] E. Praetorius, H. Poulsen, Scand. J. Clin. Lab. Invest. 5 (1953) 273–280.
[94] H. Talke, G.E. Schubert, Klin. Wochenschr. 43 (1965) 174–175.
[95] H. Bartels, M. Bohmer, C. Heierli, Clin. Chim. Acta 37 (1972) 193–197.
[96] J.I. Peterson, D.S. Young, Anal. Biochem. 23 (1968) 301–316.
[97] P. Roeschlau, E. Bernt, W. Gruber, Z. Klin. Chem. Klin. Biochem. 12 (1974) 226–232.
[98] H. Sugiuchi, Y. Uji, H. Okabe, T. Irie, K. Uekama, N. Kayahara, K. Miyauchi, Clin. Chem. 41 (1995) 717–723.
[99] J. Siedel, R. Schmuck, J. Staepels, Clin. Chem. 39 (1993) 1127.
[100] H.U. Bergmeyer, M. Horder, R.J. Rej, Clin. Chem. Clin. Biochem. 24 (1986) 481–495.
[101] A. Belfield, D.M. Goldberg, Enzyme 12 (1971) 561–573.
[102] B.T. Doumas, W.A. Watson, H.G. Biggs, Clin. Chim. Acta 31 (1971) 87–96.
[103] M.M. Bradford, Anal. Biochem. 72 (1976) 248–254.